

Elevated Testosterone Induces Apoptosis in Neuronal Cells*

Received for publication, April 4, 2006, and in revised form, June 20, 2006. Published, JBC Papers in Press, June 27, 2006, DOI 10.1074/jbc.M603193200

Manuel Estrada^{1,2}, Anurag Varshney¹, and Barbara E. Ehrlich³

From the Departments of Pharmacology and Cellular and Molecular Physiology, Yale University, New Haven, Connecticut 06520

Testosterone plays a crucial role in neuronal function, but elevated concentrations can have deleterious effects. Here we show that supraphysiological levels of testosterone (micromolar range) initiate the apoptotic cascade. We used three criteria, annexin V labeling, caspase activity, and DNA fragmentation, to determine that apoptotic pathways were activated by testosterone. Micromolar, but not nanomolar, testosterone concentrations increased the response in all three assays of apoptosis. In addition, testosterone induced different concentration-dependent Ca²⁺ signaling patterns: at low concentrations of testosterone (100 nM), Ca²⁺ oscillations were produced, whereas high concentrations (1–10 μM) induced a sustained Ca²⁺ increase. Elevated testosterone concentrations increase cell death, and this effect was abolished in the presence of either inhibitors of caspases or the inositol 1,4,5-trisphosphate receptor (InsP₃R)-mediated Ca²⁺ release. Knockdown of InsP₃R type 1 with specific small interfering RNA also abolished the testosterone-induced cell death and the prolonged Ca²⁺ signals. In contrast, knockdown of InsP₃R type 3 modified neither the apoptotic response nor the Ca²⁺ signals. These results support our hypothesis that elevated testosterone alters InsP₃R type 1-mediated intracellular Ca²⁺ signaling and that the prolonged Ca²⁺ signals lead to apoptotic cell death. These effects of testosterone on neurons will have long term effects on brain function.

Neurosteroids have been implicated as components essential for the normal function of the central nervous system (1–4). The gonadal steroid hormones are required for reproductive function, but androgens also affect areas of the brain that are not primarily involved in reproduction such as the hippocampus (5), preoptic area, amygdala, and medial hypothalamic area (6). At physiological levels, androgens are involved in neuronal differentiation, neuroprotection, neuronal survival and development (7–9). These responses occur slowly (over hours) and are mediated through the intracellular androgen receptor. In the developing brain, androgens are capable of changing the ultrastructural characteristics of the neuronal plasma mem-

brane with a relatively fast pace (10, 11). Recently, we have shown that nanomolar levels of testosterone induce rapid intracellular Ca²⁺ increases in neuroblastoma cells (within seconds), which begin as Ca²⁺ transients in the cytosol, propagate as waves of Ca²⁺ in the cytoplasm and nucleus, and develop into an oscillatory pattern (12). These Ca²⁺ signals depend on an interplay between Ca²⁺ efflux from the endoplasmic reticulum through inositol 1,4,5-trisphosphate-sensitive Ca²⁺ release channels (InsP₃Rs)⁴ and Ca²⁺ reuptake into the endoplasmic reticulum by Ca²⁺ pumps. This new testosterone-induced pathway in neuronal cells leads to neurite outgrowth (12), an essential event in neuronal differentiation (13). These results suggest an important physiological mechanism for the action of testosterone in neurons at physiological concentrations. However, it is unknown how these cells respond to high plasma levels of this neurosteroid, generally administered exogenously to achieve an increase in muscle mass (14, 15) or for replacement therapy (16). *In vivo* administration of large doses of androgens has been correlated with neurobehavioral changes like hyperexcitability, supra-aggressive nature, and suicidal tendencies (17, 18). These behavioral changes could be the outward manifestation of neuronal damage resulting from exposure to high concentrations of testosterone.

In this investigation, we evaluated the hypothesis that high concentrations of testosterone can induce deleterious effects in neurons. We show that high levels of testosterone initiate an apoptotic program in neuroblastoma cells. Apoptosis is the normal and controlled process of cell death (19). Precise control of apoptosis is critical in many processes of life, including development and disease. The onset of apoptosis and its progression can be altered by both endogenous and exogenous insults (20). Apoptosis is characterized by many physical, cellular, and physiological parameters, which include membrane blebbing, caspase activation, change in membrane potential, and DNA damage-associated nuclear deformation (19, 21, 22). Prolonged elevated cytosolic calcium (Ca²⁺) concentrations can initiate the apoptotic program in many cell types (23, 24), including neurons (25). The testosterone-induced apoptosis described here occurs through overactivation of intracellular Ca²⁺ signaling pathways. The progression into cell death could be attenuated by the addition of inhibitors of the InsP₃R signaling pathway. Moreover, we found that InsP₃R type 1, the predominant isoform of the InsP₃R found in neurons (26), is the key integrator of the testosterone response in both normal and

* This work was supported by National Institutes of Health Grants GM63496 and DK61747 (to B. E. E.), and FONDECYT Grant 1060077 (to M. E.), and a National Kidney Foundation postdoctoral fellowship (to A. V.). The costs of publication of this article were defrayed in part by the payment of page charges. This article must therefore be hereby marked "advertisement" in accordance with 18 U.S.C. Section 1734 solely to indicate this fact.

¹ These authors contributed equally to this work.

² Present address: Programa de Fisiología y Biofísica, ICBM, Facultad de Medicina, Universidad de Chile, Correo 7, Santiago, Chile. Tel.: 56-2-9786272; Fax: 56-2-7776916; E-mail: iestrada@med.uchile.cl.

³ To whom correspondence should be addressed: Dept. of Pharmacology, Yale University, 333 Cedar St., New Haven, CT 06520-8066. Tel.: 203-737-1158; Fax: 203-737-2027; E-mail: barbara.ehrlich@yale.edu.

⁴ The abbreviations used are: InsP₃R, inositol 1,4,5-trisphosphate receptor; XTT, 3-(4,5-dimethylthiazol-2-yl)-2,5-diphenyltetrazolium bromide salt; PBS, phosphate-buffered saline; Ac, N-acetyl; AFC, amino-4-trifluoromethyl coumarin; CHO, aldehyde; pNA, p-nitroanilide; 2-APB, 2-aminoethyl diphenylborate; siRNA, small interfering RNA.

hyperstimulated Ca^{2+} signaling in neuroblastoma cells. It is this pathway that has been implicated in other pathophysiological conditions. For example, overstimulation of the apoptotic program in neurons has been associated with several neurological illnesses, such as Alzheimer disease (27, 28) and Huntington disease (29–31). Our results suggest that the responses to elevated testosterone can be compared with these pathophysiological conditions.

MATERIALS AND METHODS

Chemical Reagents—Testosterone, 17β -estradiol, 2-aminoethoxydiphenyl borate (2-APB), and the TOX-2 cell viability assay were purchased from Sigma. Fluo4-acetoxymethyl ester was acquired from Molecular Probes, Inc. (Eugene, OR). Caspase-cleavable peptides, Ac-DEVD-AFC and Ac-DEVD-CHO, were obtained from BD Biosciences. Cell-permeable forms of these peptides, colorimetric caspase substrate Ac-DEVD-pNA, and xestospongine-C were obtained from Calbiochem.

Cell Cultures—The human neuroblastoma cell line (SH-SY5Y; ATCC) was cultured in 1:1 Dulbecco's modified Eagle's medium/Ham's F-12 medium supplemented with 10% (v/v) heat-inactivated fetal bovine serum, 5% nonessential amino acids, 100 units of penicillin, and 50 $\mu\text{g}/\text{ml}$ streptomycin in a 95% air, 5% CO_2 humidified incubator at 37 °C. Cells were grown on 22 \times 22-mm gelatin-coated glass coverslips for the Ca^{2+} measurements or in 100-mm Petri dishes for biochemical and spectrochemical assays. Cultured cells were washed once with PBS before stimulation with testosterone (from concentrated stocks made in ethanol). The final ethanol concentration (<0.01%) had no effect on intracellular Ca^{2+} concentration or biochemical determinations (32).

Cell Viability—Cells were exposed to various concentrations of steroid hormones for different times. The number of viable cells was determined using a standard trypan blue exclusion assay. Cells were washed twice with PBS and then resuspended with EDTA. Cells were stained with 0.5% trypan blue, and the number of viable and nonviable cells was determined in a hemacytometer. Results are expressed as percentage viability ($100 \times$ number of viable cells/number of total cells per well) for each concentration of hormone tested. Cell viability was also assessed using the TOX-2 kit (Sigma) according to the manufacturer's protocol. This method determines the ability of metabolically active cells to reduce the yellow salt 3-(4,5-dimethylthiazol-2-yl)-2,5-diphenyltetrazolium bromide (XTT) to an orange formazan dye. Therefore, the conversion only occurs in living cells, and the amount of orange formazan formed directly correlates to the number of living cells. Neuroblastoma cells, grown in 60-mm Petri dishes in culture medium without phenol red and exposed to different steroid hormone concentrations, were washed with PBS and incubated with the XTT solution (final concentration 0.3 mg/ml), according to the kit specifications. After this incubation period, quantification of formazan dye formed was determined using a spectrophotometer at a wavelength of 450 nm minus the absorbance at 690 nm. Results are expressed as percentages with respect to controls (untreated cells).

Ca^{2+} Imaging—Cells were loaded with 5 μM Fluo4-acetoxymethyl ester at 37 °C for 30 min in "imaging solution": 135 mM NaCl, 5 mM KCl, 2 mM MgCl_2 , 2 mM CaCl_2 , 10 mM HEPES, 5.6 mM glucose, pH 7.4. After loading, cells were washed twice with the imaging solution and placed on an inverted microscope (Axiovert 100; Zeiss) connected to a laser scanning imaging system (LSM 510 META; Zeiss). Cells were stimulated with the hormone diluted in the imaging solution. A 488-nm excitation wavelength was focused through a 40 \times Apochromat water immersion objective lens (numerical aperture 1.2; Zeiss). In order to identify the cells expressing the siRNA, cells were cotransfected with DsRed-pCMV-cyto construct, which produced DsRed (red fluorescence protein), and were examined using fluorescence excitation at 568 nm. Regions of interest with the same pixel dimensions were identified and analyzed using Image J software (National Institutes of Health, Bethesda, MD). The inhibitors were added during the dye incubation; times and concentrations are indicated under "Results." The fluorescence intensity ratio (F/F_0) was plotted as a function of time.

Annexin V Labeling—Cells were incubated in different concentrations of testosterone for 6 h. After treatment, cells were washed twice with PBS and once with fixation buffer (10 mM HEPES/NaOH, pH 7.4, 140 mM NaCl, 5 mM CaCl_2) and were incubated with fluorescein isothiocyanate-conjugated annexin V (0.5 μl per 100 μl of fixation buffer; BD Biosciences) for 15 min at room temperature. The fluorescence of fluorescein isothiocyanate was visualized by laser-scanning confocal microscopy (LSM 510 META; Zeiss). Annexin V fluorescence-positive cells were analyzed by the Image J program using the particle analysis macro (National Institutes of Health) and normalized to total cell count.

DNA Fragmentation Assay—Neuroblastoma cells (1×10^6 cells) growing on 100-mm plates were washed once in PBS, harvested in 0.5 ml of extraction buffer (50 mM Tris-HCl, pH 8.0, 10 mM EDTA, 0.5% SDS, 0.5 mg/ml proteinase K), and incubated at 55 °C for 30 min in the presence of 20 mg/ml RNase A. The lysate was centrifuged at $15,000 \times g$ for 10 min, and aqueous fractions were extracted with phenol/chloroform two to three times. Nucleic acids were precipitated with 0.1 volumes of 3 M sodium acetate and 2.5 volumes of 100% ethanol. Pelleted DNA was washed with 70% ethanol and was resuspended in TE buffer (10 mM Tris-HCl, 1 mM EDTA, pH 8.0) kept at 37 °C. DNA was run on a 2% agarose gel containing ethidium bromide, visualized with a UV transilluminator, recorded with a UVP gel-doc system, and analyzed by scanning densitometry.

Assay of Proteolytic Activity of Caspases—6 h after incubation with 100 nM to 10 μM testosterone, 1×10^6 neuroblastoma cells were washed with PBS and collected in cell lysis buffer (50 mM HEPES, pH 7.5, containing 10% sucrose and 1% Triton X-100). Following removal of cell debris and mitochondria from the lysate by centrifugation, the supernatant was diluted 2-fold with PBS and incubated at 37 °C for 30 min in the presence of 10 mM dithiothreitol. Ac-DEVD-AFC (at the final concentration of 15 μM), dissolved in Me_2SO , was added to the mixture, and the sample was incubated for another 30 min. The mixture was then transferred to a quartz 1-cm square cuvette,

Testosterone-induced Neuronal Apoptosis

and AFC fluorescence (excitation, 400 nm; emission, 505 nm) was measured (Quantmaster spectrofluorometer; Photon Technology International). For colorimetric measurement of caspase activity, Ac-DEVD-*p*NA (Calbiochem) was added at a final concentration of 200 μ M to lysates generated from identical numbers of cells under different experimental conditions. Caspase activity was monitored as optical absorbance at 405 nm (Spectronic Genesys2 spectrophotometer) in a time-dependent manner. In the caspase inhibition experiments, 200 nM Ac-DEVD-CHO (BD Biosciences) was added to the mixture prior to Ac-DEVD-AFC or Ac-DEVD-*p*NA for 30 min.

Western Blot—Cells lysates containing 40 μ g of protein were separated by SDS-PAGE in a 4–20% linear gradient followed by electrophoretic transfer onto polyvinylidene difluoride membranes for 3 h at 400 mA. The following primary antibodies and their dilution were used: anti-InsP₃R type 1 (1:2,000; custom produced by Research Genetics), anti-InsP₃R type 3 (1:1,000; BD Biosciences), ERK2 (1:1,000, Santa Cruz Biotechnology, Inc., Santa Cruz, CA). Membranes were incubated with primary antibodies overnight at 4 °C. After incubation with horseradish peroxidase-conjugated secondary antibodies (1:10,000; Bio-Rad) for 2 h at room temperature, the bands were visualized by an enhanced chemiluminescence system (Pierce). Membranes were stripped and reprobed with ERK2 antibody, which was used as a sample loading control. Blots were quantified by scanning densitometry.

siRNA—siRNAs for InsP₃R type 1 and type 3 were kindly provided by Dr. M. Nathanson (Yale University). The siRNA templates were obtained from Ambion, and the sequence was AAAGCACCAGCAGCTACAACCTCCTGTCTC of the human InsP₃R type 1 and AAACAAGTTTGCCAGCACCAT for InsP₃R type 3. Transfection of cells with siRNA was performed using RNAiFect (Qiagen), and down-regulation of either type 1 or type 3 InsP₃R was confirmed by immunofluorescence and Western blot analysis.

Statistics—Data are expressed as the mean \pm S.E. Colorimetric measurements of caspase activity were fit to a linear equation to estimate the rate of activation. In order to compare the difference between basal and poststimulated points, we carried out analysis of variance, and the statistic differences were determined by the Bonferroni post-test. $p < 0.05$ was considered statistically significant.

RESULTS

High Concentration of Testosterone Induces Neurotoxicity—Previously we found that physiological concentrations of testosterone (nanomolar range) induced neuronal differentiation in neuroblastoma cells (12), but it was not clear that supraphysiological levels of this hormone (micromolar range) would have the same effect. Therefore, we treated neuroblastoma cells with different concentrations of testosterone and compared the effect on several parameters, including cell survival. When treated with low concentrations of testosterone (100 nM), cell viability did not change to any appreciable extent over the time range studied (Fig. 1A). Exposure of the cells to 1 μ M testosterone induced a significant decrease in cell viability over 24 h. At 10 μ M, testosterone was even more lethal (Fig. 1A). To confirm the results determined by the trypan blue exclusion assay, we

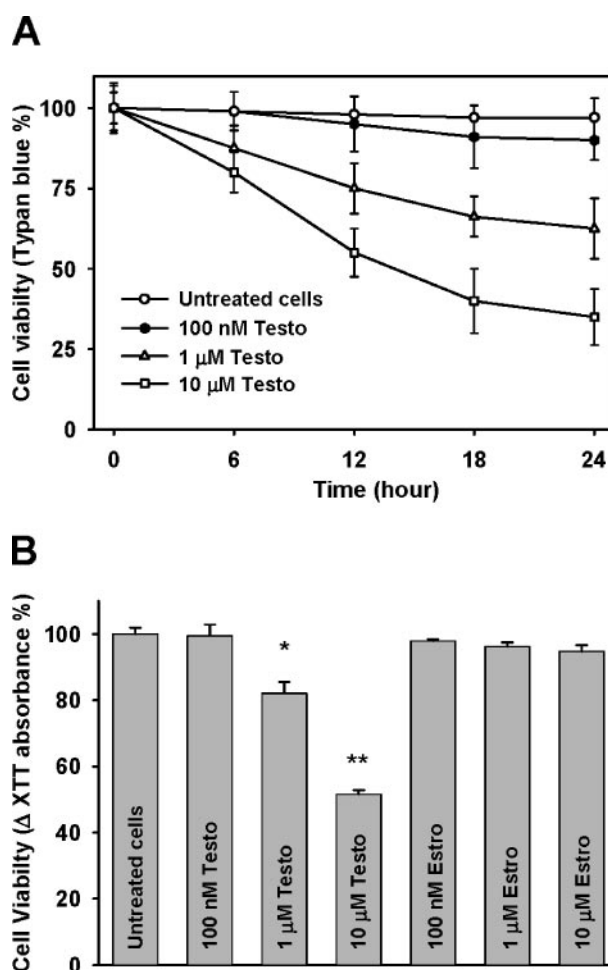


FIGURE 1. High concentrations of testosterone cause cytotoxicity in neuroblastoma cells. A, time course of neuroblastoma cell survival as a function of various testosterone concentrations. Cells were incubated with 100 nM (●), 1 μ M (△), or 10 μ M (□) of testosterone (*Testo*) for the indicated times. Untreated cells were used as a negative control (○). Cell viability was assessed for trypan blue exclusion (where 100% is complete exclusion), and data were averaged for 1×10^6 cells. B, cells were treated with various concentrations of either testosterone or 17 β -estradiol (*Estro*) and were scored for viability using an XTT assay 12 h after treatment with the hormones. The values represent the mean \pm S.E. of three independent experiments. (*, $p < 0.05$; **, $p < 0.01$).

monitored the effect of testosterone using the XTT cell viability assay. The response after 12 h of treatment was selected for comparison, because the higher concentrations of testosterone (1 and 10 μ M) induced a significant deleterious effect at this time point using the previous assay. As predicted, 100 nM testosterone did not affect cell viability, whereas 1 and 10 μ M testosterone significantly decreased cell viability (Fig. 1B). Using a similar range of concentrations of estrogen (17 β -estradiol), we saw no effect on cell viability, indicating that the decrease in cell viability was specifically triggered by high concentrations of testosterone (Fig. 1B).

High Concentrations of Testosterone Induce Apoptosis—Cell viability as determined using either trypan blue exclusion or XTT methods does not discriminate between cell death by apoptosis or necrosis. To identify the mechanism of cell death induced by testosterone, we examined annexin V labeling, caspase activation, and DNA laddering, all markers of apoptosis. Untreated cells did not show fluorescence due to annexin V

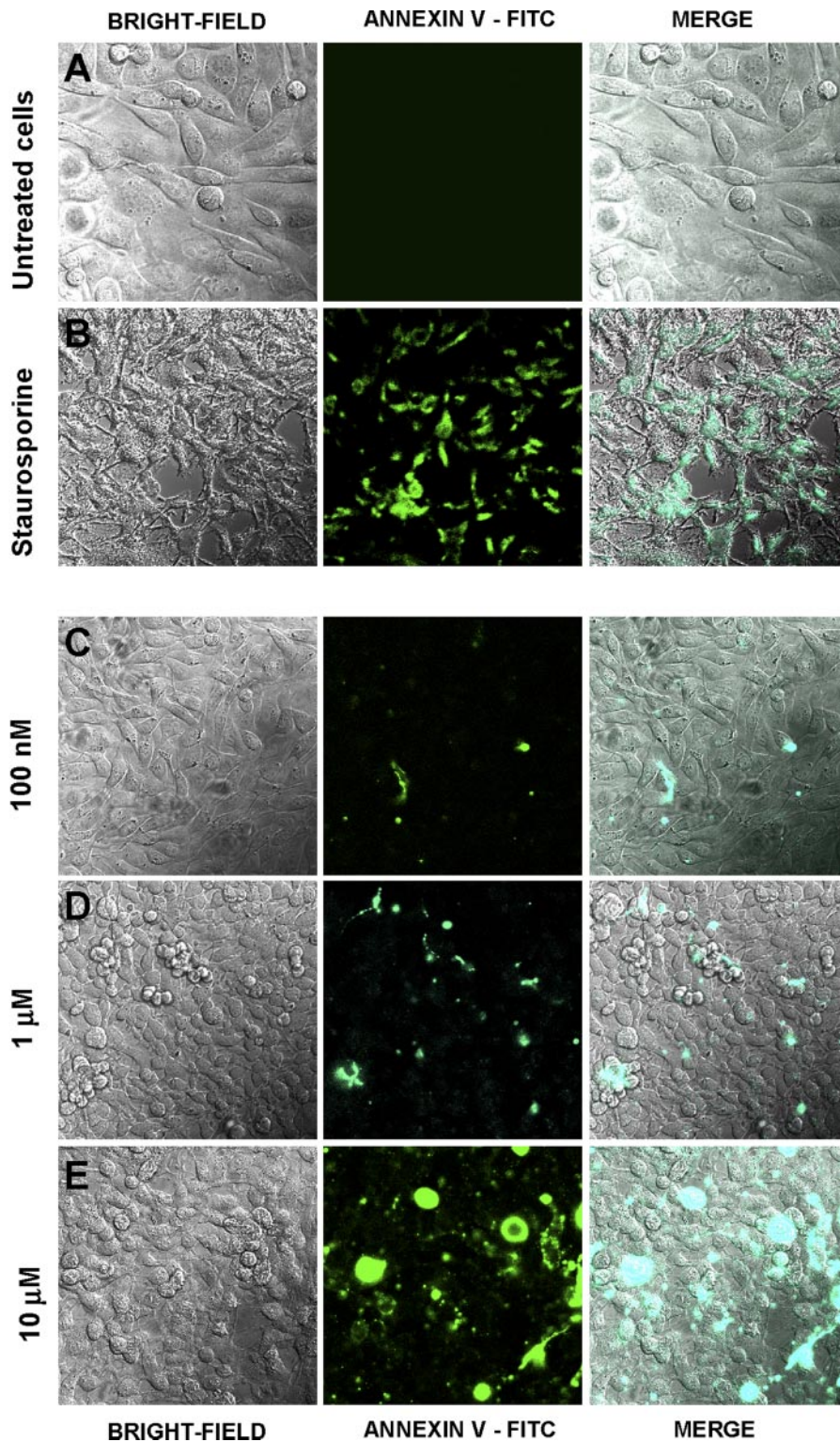


FIGURE 2. Effect of testosterone on annexin V labeling in neuroblastoma cells. Cells were exposed to different concentrations of testosterone and the fluorescent apoptotic marker, annexin V, was visualized by confocal microscopy. *A*, untreated cells did not show fluorescence, and in the bright field image the integrity of the cells was observed. *B*, staurosporine was used as a positive control to maximally induce apoptosis. Cells induced with $1 \mu\text{M}$ staurosporine displayed a high fluorescence with a marked change in the cellular morphology. *C–E*, cells were exposed to three concentrations of testosterone for 12 h, and the annexin V-positive labeling was determined. *C*, at 100 nM testosterone, few cells were positive to annexin V, and the cell morphology did not change when compared with the control cells. At $1 \mu\text{M}$ (*D*) and $10 \mu\text{M}$ (*E*) testosterone, an increase in the number of fluorescent cells was observed. In the bright field images, cells were much rounder in shape with loss of their process. For each concentration, at least 1000 cells were counted. *, $p < 0.05$. FITC, fluorescein isothiocyanate.

labeling (Fig. 2*A*), whereas staurosporine ($1 \mu\text{M}$), a well established inducer of apoptosis, produced high levels of annexin V-positive cells, depicted in green (Fig. 2*B*). In the bright field image, it is possible to observe the morphological changes induced by staurosporine (Fig. 2*B*; *superimposed images* are shown in the *right panel*). When neuroblastoma cells were exposed to 100 nM testosterone, very few annexin V-positive cells were detected after 6 h of incubation (Fig. 2*C*; $4 \pm 1\%$, $n = 780$ cells). Elevated concentrations of testosterone significantly increased the number of annexin V-positive cells: $21 \pm 3\%$ for $1 \mu\text{M}$ ($n = 834$ cells; $p < 0.05$) and 34 ± 8 for $10 \mu\text{M}$ ($n = 600$ cells; $p < 0.01$) testosterone were annexin V-positive (Fig. 2, *D* and *E*), where p values are calculated for treatment as compared with the control. These percentages for apoptotic cell death are consistent with the number of dead cells identified by the cell viability assay. Moreover, bright field images also show morphological changes associated with apoptosis; cells have plasma membrane blebs and were more round in shape with loss of their processes (Fig. 2, *D* and *E*). To further confirm the specificity of the response to testosterone, cells were exposed to high concentrations of estrogen (1–10 μM). There was no significant labeling of annexin V detected (data not shown), indicating that the apoptotic death pathway was specifically activated by testosterone.

Apoptotic cell death can be defined by morphological and biochemical characteristics, such as DNA fragmentation (33), that can be visualized on an agarose gel. We observed that 1 and 10 μM testosterone induced considerable DNA damage in neuroblastoma cells within 6 h (Fig. 3*A*, lanes 4 and 5), whereas treatment with 100 nM testosterone for the same duration did not induce DNA damage (Fig. 3*A*, lane 3). To be certain that the death of neuroblastoma cells is indeed due to a canonical apoptotic pathway, it is necessary to show that testoster-

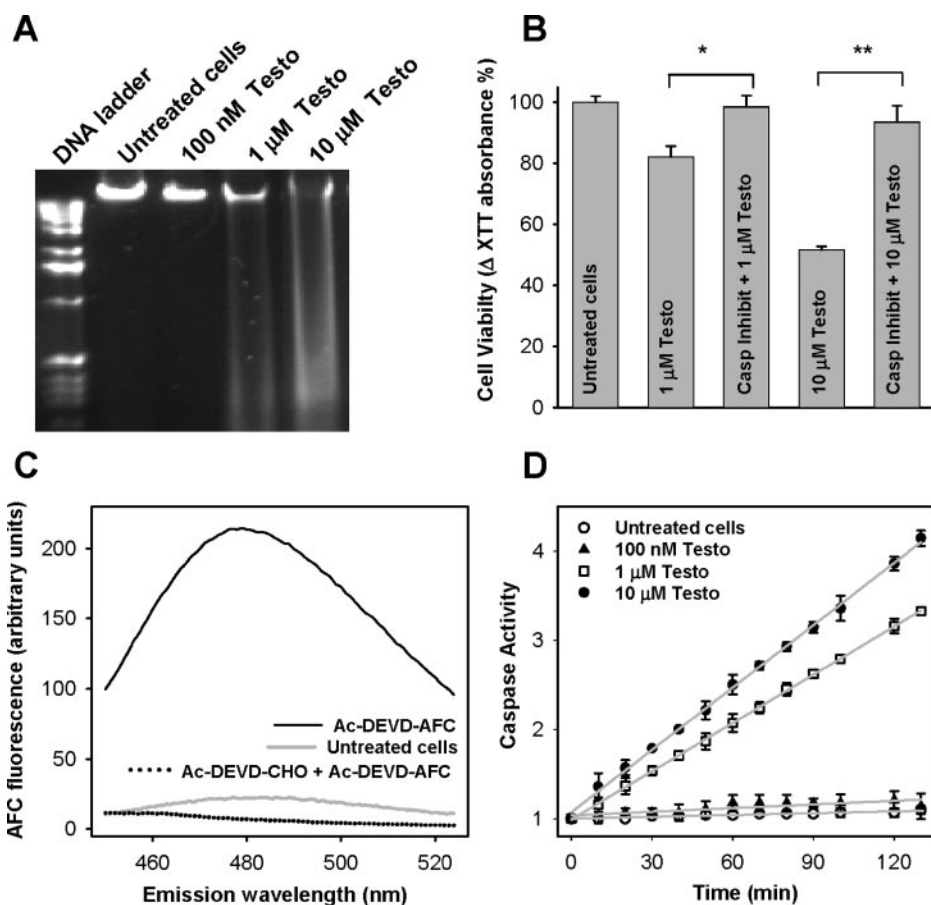


FIGURE 3. DNA fragmentation and assay of caspase activity in neuroblastoma cells. *A*, cells were treated with three concentrations of testosterone (*Testo*) for 6 h, and DNA fragmentation was assessed by 2% agarose gel electrophoresis and ethidium bromide staining. *B*, neuroblastoma cell viability was determined by an XTT assay. Cells were preincubated with the cell-permeable caspase inhibitor and exposed to 1 μM or 10 μM testosterone for 12 h. *C*, the fluorescence spectrum, recorded 30 min after the addition of Ac-DEVD-AFC to the extract prepared from 1 μM testosterone-induced cells. Ac-DEVD-AFC was added to a final concentration of 150 nM. The caspase-dependent release of AFC following hydrolysis of the substrate is monitored upon excitation at 400 nm. A distinctive emission peak was observed between 475 and 505 nm. The extracts were prepared from 1 × 10⁶ cells ~6 h after treatment with testosterone (*black line*) or from cells without any treatment (*gray line*). The addition of the caspase inhibitor Ac-DEVD-CHO competitively blocked the AFC release. Lysates from the testosterone-treated cells that were incubated first with Ac-DEVD-CHO and then subjected to the same treatment as in *C* did not exhibit the AFC release (*dotted line*). *D*, concentration dependence of testosterone on caspase activation. For these experiments, a colorimetric substrate of caspase, Ac-DEVD-pNA, was used. Lysates generated from cells treated with 100 nM (▲), 1 μM (□), and 10 μM (●) testosterone were incubated with the substrate, and the pNA absorbance was plotted as a function of time. Lysates from untreated cells were used as negative control (○). Data points were fit to a straight line (*gray lines*) to calculate the rate of caspase activation (1.1 ± 0.05/s and 1.4 ± 0.02/s for 1 and 10 μM testosterone treatments, respectively). The same amount of protein was used in each assay. The values represent the mean ± S.E. of three independent experiments (*, *p* < 0.05; **, *p* < 0.01).

one activates aspartate-specific proteases (caspases) (34). Pre-treatment of neuroblastoma cells with the cell-permeable caspase inhibitor (Ac-DEVD-CHO with 16 N-terminal amino acid residues of the signal peptide of Kaposi fibroblast growth factor that confers cell permeability to the peptide) abolishes the testosterone effect on cell viability at both concentrations tested earlier (Fig. 3*B*). To directly follow caspase activity, the hydrolysis of a specific fluorogenic substrate, Ac-DEVD-AFC, in cell-free extracts prepared from neuroblastoma cells was recorded after cells were treated with testosterone. The steady-state fluorescence emission spectrum of the mitochondria-free extract (Fig. 3*C*), recorded after the addition of Ac-DEVD-AFC, indicates hydrolysis of the substrate and release of the AFC fluorophore. Prior addition of the caspase inhibitor, Ac-

DEVD-CHO, competitively inhibits AFC release (Fig. 3*C*), suggesting the specific activation of aspartate protease(s). The cell-free extracts prepared from untreated neuroblastoma cells produced no caspase activity. In addition, the time course of caspase activation as a function of increasing concentrations of testosterone was monitored by using a colorimetric caspase substrate Ac-DEVD-pNA. There was an increase in caspase activity in cells treated with either 1 or 10 μM testosterone, whereas treatment with 100 nM testosterone elicited caspase activity comparable with that of untreated cells (Fig. 3*D*). All three characteristic parameters, annexin V labeling, DNA fragmentation, and caspase activation, were induced by treatment with testosterone, supporting the conclusion that cells treated with high levels of testosterone (micromolar concentrations) die by initiation of the apoptotic cascade.

High Concentrations of Testosterone Increase Intracellular Ca²⁺—An incremental rise in cytosolic Ca²⁺ has been suggested as a critical step in activating neuronal apoptosis (22). We examined the testosterone-induced Ca²⁺ responses in neuroblastoma cells by measuring Ca²⁺ changes at the single cell level in cells loaded with the Ca²⁺-sensitive fluorescent dye, Fluo4-acetoxymethyl ester. Stimulation of neuroblastoma cells with different testosterone concentrations (100 nM, 1 μM, and 10 μM) induced Ca²⁺ responses with different temporal patterns (Fig. 4). At 100 nM testosterone, increases in Ca²⁺, which

were absent at the time of hormone application, were observed, and the level of Ca²⁺ returned to the basal level between repetitive oscillations (Fig. 4*A*; *n* = 70 cells from five independent cultures). We previously determined that Ca²⁺ signals evoked by testosterone were dependent on the generation of inositol 1,4,5-trisphosphate as well as on the activity of the InsP₃R (12). At higher concentrations of testosterone, the response was more irregular, often with a persistent Ca²⁺ rise, which was maintained as long as hormone was present in the medium. At 1 μM, an initial rise was observed that was followed by a slow return to base line (Fig. 4*B*, *n* = 83 cells, from four independent cultures), whereas at 10 μM, long lasting Ca²⁺ increases were seen where the return to basal level occurred only after several minutes (Fig. 4*C*, *n* = 91 cells, from four independent cultures).

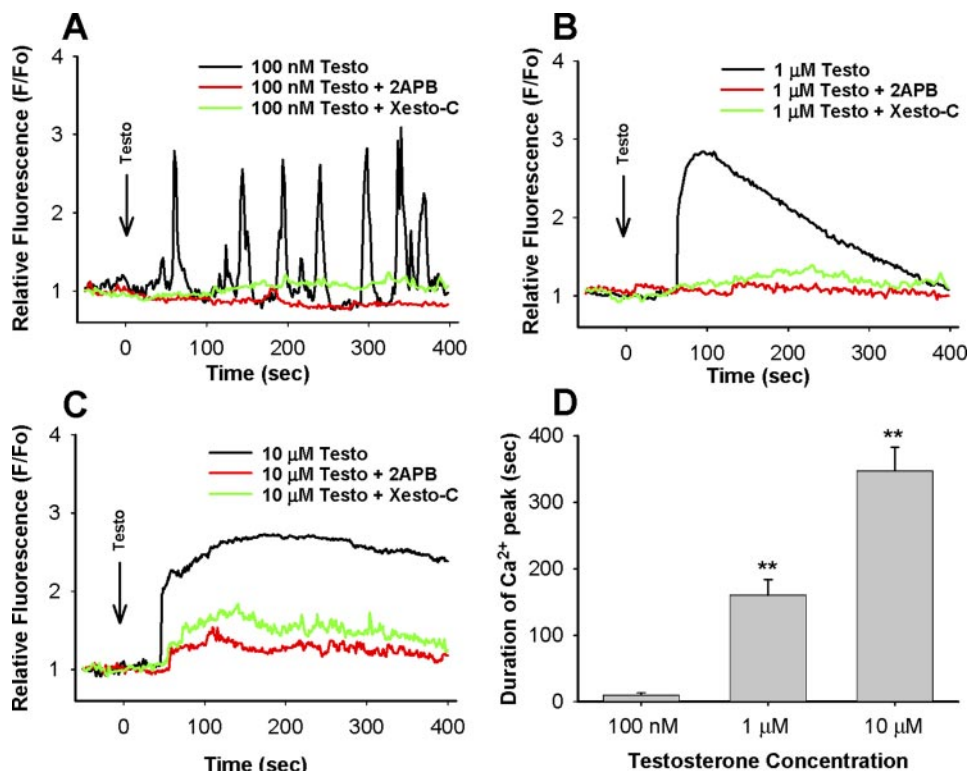


FIGURE 4. Testosterone induces rises in intracellular Ca^{2+} in a concentration-dependent manner. The relative fluorescence change (ratio between stimulated and basal values) as a function of time is shown for three different concentrations of testosterone. Shown are representative single cell intracellular Ca^{2+} tracings in response to the indicated hormone concentrations; the arrows indicate the time of stimulation. Three types of responses were observed; nanomolar concentrations of testosterone induced Ca^{2+} oscillations (A), whereas micromolar concentrations produced long lasting Ca^{2+} transients (B and C) without oscillations. The testosterone-induced Ca^{2+} response was blocked, at all three concentrations of testosterone, in cells preincubated with inhibitors of the InsP_3R , 2-APB (20 μM), or xestospongine-C (Xesto-C; 5 μM). D, each bar corresponds to the average duration of a Ca^{2+} response (or transient) of a single cell evoked by a specific concentration of testosterone. The bars indicate mean \pm S.E. of ~ 50 individual cells from six independent experiments. *, $p < 0.05$; **, $p < 0.01$.

The duration of the Ca^{2+} spike increased as the hormone concentration was raised (Fig. 4D), showing a change from repetitive Ca^{2+} spikes to a prolonged Ca^{2+} transient. The peak amplitudes of the Ca^{2+} transients were conserved (Fig. 4). These results demonstrate a loss of the normal oscillatory Ca^{2+} pattern when testosterone levels are elevated.

The ability of testosterone to induce either Ca^{2+} oscillations or sustained Ca^{2+} responses was attenuated by InsP_3R inhibitors. When the cells were preincubated with either 2-APB (20 μM) or xestospongine-C (5 μM), the testosterone-induced Ca^{2+} oscillations at 100 nM were abolished (Fig. 4A; $n = 46$ and $n = 57$, respectively). The addition of InsP_3R inhibitors also altered the Ca^{2+} response patterns evoked by elevated concentrations of testosterone. At 1 or 10 μM testosterone, the Ca^{2+} response was significantly attenuated or inhibited (Fig. 4, B and C; $n = 35$ and $n = 48$, respectively). Taken together, these results suggest that testosterone regulates InsP_3R -evoked Ca^{2+} increases by controlling the Ca^{2+} release from internal stores.

InsP₃R Is Involved in the Apoptotic Pathway Induced by Testosterone—Our results suggest that the InsP_3R is directly involved in the apoptotic response induced by testosterone. We tested this hypothesis by monitoring the apoptosis parameters in the presence of InsP_3R blockers. Cells treated with 1 or 10 μM testosterone in the presence of these blockers had significantly

lower staining for annexin V as compared with cells treated with testosterone alone (compare Fig. 5, A and B, with Fig. 2, D and E). We found that 2-APB and xestospongine-C could also protect the cells from apoptosis-associated DNA damage (Fig. 5C, lanes 3 and 4, and Fig. 5D). We also compared caspase activity in the presence of 2-APB and xestospongine-C and found that treatment with InsP_3R blockers suppressed the activation of caspases by testosterone at both concentrations tested (see Fig. 5E for 1 μM). The rates of caspase activation by testosterone were significantly lower when cells were treated with 2-APB and xestospongine-C (Fig. 5F). Taken together, these results confirm that testosterone-induced apoptosis is mediated through InsP_3R and that InsP_3R blockers can protect cells from progression into this cell death pathway.

InsP₃R Type 1 Is Involved in Both Normal and Dysregulated Ca^{2+} Signaling—Neuroblastoma cells express mainly InsP_3R type 1 (35), but the presence of significant amounts of InsP_3R type 3 has also been described (36). To establish which isoform of InsP_3R is important for the testosterone-induced

Ca^{2+} increases and subsequent activation of the cell death program, neuroblastoma cells were transfected with specific siRNA against InsP_3R type 1 or type 3. These siRNA probes have not shown any cross-reactivity among the subtypes (37). There was a significant reduction in the immunosignal for InsP_3R protein in either InsP_3R type 1 siRNA-transfected cells (Fig. 6A, left; $n = 6$; $p < 0.01$) or InsP_3R type 3 siRNA-transfected cells (Fig. 6A, right; $n = 6$; $p < 0.01$). Cells knocked down for InsP_3R type 1 or type 3 were then treated with testosterone under conditions described earlier. Cells knocked down for InsP_3R type 3 showed a similar caspase activity as untransfected cells, whereas in cells knocked down for InsP_3R type 1, the caspase activity induced by 1 μM testosterone was completely abolished (Fig. 6B). In order to determine the molecular contribution of InsP_3R type 1 and type 3 to the testosterone-induced Ca^{2+} response, Ca^{2+} transients were recorded in InsP_3R type 1 or type 3 knocked down cells. To identify the successfully transfected cells, we co-transfected the siRNA with a plasmid DNA coding for DsRed. We found that neuroblastoma cells knocked down for InsP_3R type 3 did not modify their ability to evoke Ca^{2+} oscillations or prolonged transients in response to testosterone (Fig. 6, C–E, black lines). These responses to testosterone were similar to those recorded in untransfected cells (compare Fig. 6, C–E, with Fig. 4). In contrast, cells knocked down for

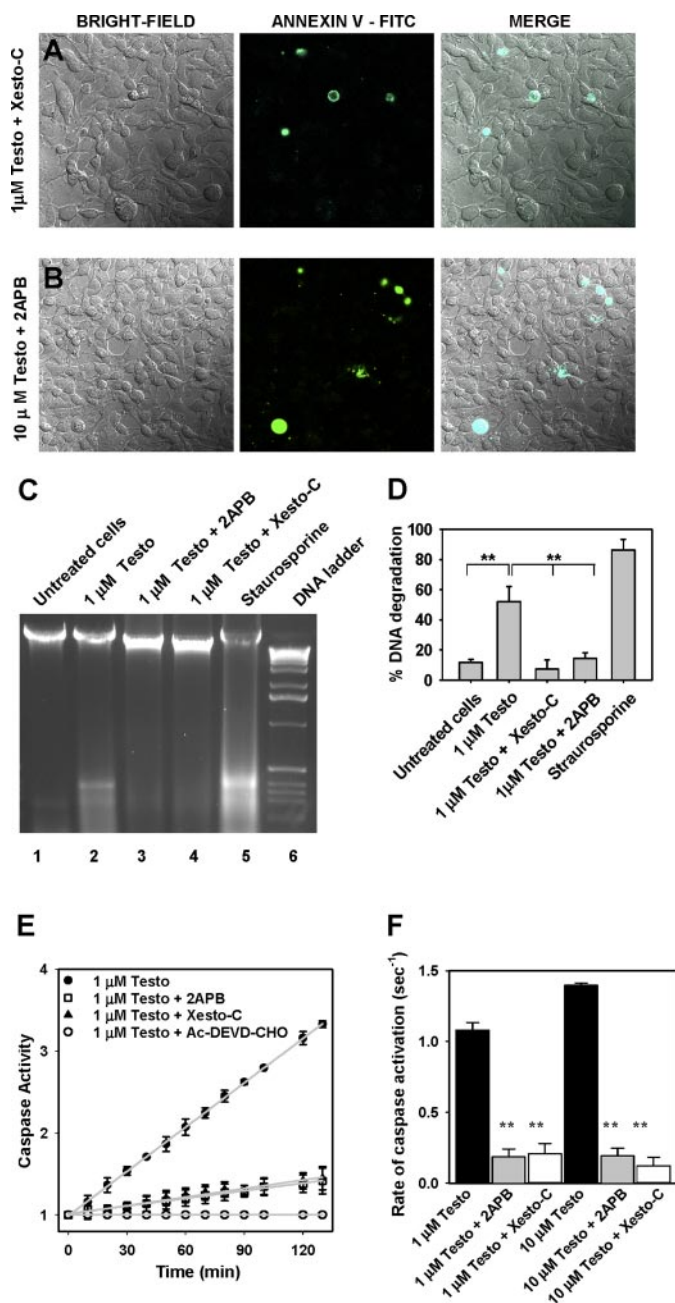


FIGURE 5. *InsP₃R* blockers inhibit testosterone-induced apoptosis. Inhibitors of *InsP₃R*, 2-APB (20 μM), and xestospongine-C (*Xesto-C*; 5 μM) were used to determine the role of the *InsP₃R* in testosterone-induced apoptosis. *A* and *B*, annexin V labeling in the presence of *InsP₃R* inhibitors. Cells were treated with high (1 μM (*A*)) and 10 μM (*B*)) concentrations of testosterone in the presence of 2-APB or xestospongine-C and scored for annexin V-positive cells. Upon the addition of these blockers, few cells were positive to annexin V, and the cell morphology did not change with respect to the control cells; compare these images with the responses shown in Fig. 2. One representative set of images is shown for 1 and 10 μM testosterone. *C*, DNA fragmentation in the presence of *InsP₃R* blockers. Genomic DNA isolated from neuroblastoma cells treated with 1 μM testosterone in the presence of 2-APB (*lane 3*) and *Xesto-C* (*lane 4*) show significantly less DNA damage than that of 1 μM testosterone alone (*lane 2*). Cells without treatment (*lane 1*) and cells treated with 1 μM staurosporine (*lane 5*) were used as negative and positive control experiments, respectively. DNA damage was quantified by scanning densitometry and was normalized by total DNA intensity in each *lane*. *D*, the percentage of DNA degraded by 1 μM testosterone (52 ± 11%), in the presence of 2-APB (14 ± 2%), or in the presence of xestospongine-C (8 ± 6%) with respect to the response after treatment with staurosporine (86 ± 6%) and untreated cells (12 ± 3%). *E* and *F*, testosterone-induced caspase activity in the presence of *InsP₃R* inhibitors. Using a colorimetric caspase substrate, Ac-DEVD-pNA, the

the *InsP₃R* type 1 did not respond to testosterone (Fig. 6, *C–E*, gray lines), but they still responded to extracellular application of ATP (data not shown). The magnitude of the response to thapsigargin, an inhibitor of the Ca²⁺ pump on the endoplasmic reticulum, was similar (data not shown), suggesting that store loading was unchanged by *InsP₃R* knockdown. These data indicate a critical role of *InsP₃R* type 1 but not type 3 in controlling the Ca²⁺ signaling in response to testosterone and regulation of its neuronal function.

DISCUSSION

Testosterone is the main endogenous anabolic/androgenic steroid hormone, and it plays fundamental roles in development, differentiation, and cellular growth (38, 39). In neurons, testosterone acts as a neurosteroid and can induce changes at the cellular level, which in turn lead to changes in behavior, mood, and memory (40). Both neuroprotective (41, 42) as well as neurodegenerative (43) effects of androgens have been reported. Testosterone levels are substantially increased in human subjects using elevated doses of anabolic steroids to increase muscle mass (14), which can negatively affect their behavior (17) or induce degenerative processes (40). The cellular mechanisms of these physiological and deleterious effects of testosterone have not been elucidated.

In the present study, we have demonstrated for the first time that the treatment of neuroblastoma cells with elevated concentrations of testosterone for relatively short time periods (6–12 h) induces a decrease in cell viability by activation of a cell death program. Low concentrations of testosterone had no effects on cell viability, whereas at high concentrations the cell viability decreased with incremental increases in hormone concentration. Using three characteristic parameters, it was possible to show that this action of testosterone was through the apoptotic program. Being lipid-soluble molecules, steroids could influence membrane fluidity (and phosphatidylserine accessibility), as shown in lipid bilayer experiments with millimolar concentrations of steroids (44). In addition, aromatase, an enzyme that converts testosterone into estrogen (17β-estradiol), has been reported in the central nervous system and neuroblastoma cells (45). To rule out these possibilities, we simulated the cells with estrogen and found that equally elevated concentrations of estrogen had no effect on cell viability (Fig. 1*B*), suggesting that the response was specific for elevated testosterone concentration and not due to its metabolism to estrogen (Fig. 1*B*).

Previously, we demonstrated that testosterone (10–100 nM) induces intracellular Ca²⁺ oscillations in the cytosol and nucleus, which are an important mediator of downstream

time course of caspase activation was followed in lysates from cells treated with testosterone in the presence of *InsP₃R* blockers. *E*, caspase activation induced by 1 μM testosterone (●) is inhibited by 2-APB (□) or xestospongine-C (▲) treatment. The addition of the caspase inhibitor, Ac-DEVD-CHO, also abolishes the caspase activity (○). These data were fit to the linear functions (gray lines) to yield rates of caspase activation. *F*, rates of caspase activation are severely affected by *InsP₃R* blockers at both concentrations of testosterone tested. At 1 μM testosterone, the rate of caspase activation was 1.1 ± 0.1/s versus 0.2 ± 0.2/s for 2-APB and 0.2 ± 0.1/s for xestospongine-C. At 10 μM testosterone, the rate of caspase activation was 1.4 ± 0.0/s versus 0.2 ± 0.1/s for 2-APB and 0.1 ± 0.1/s for xestospongine-C. **, *p* < 0.01. FITC, fluorescein isothiocyanate.

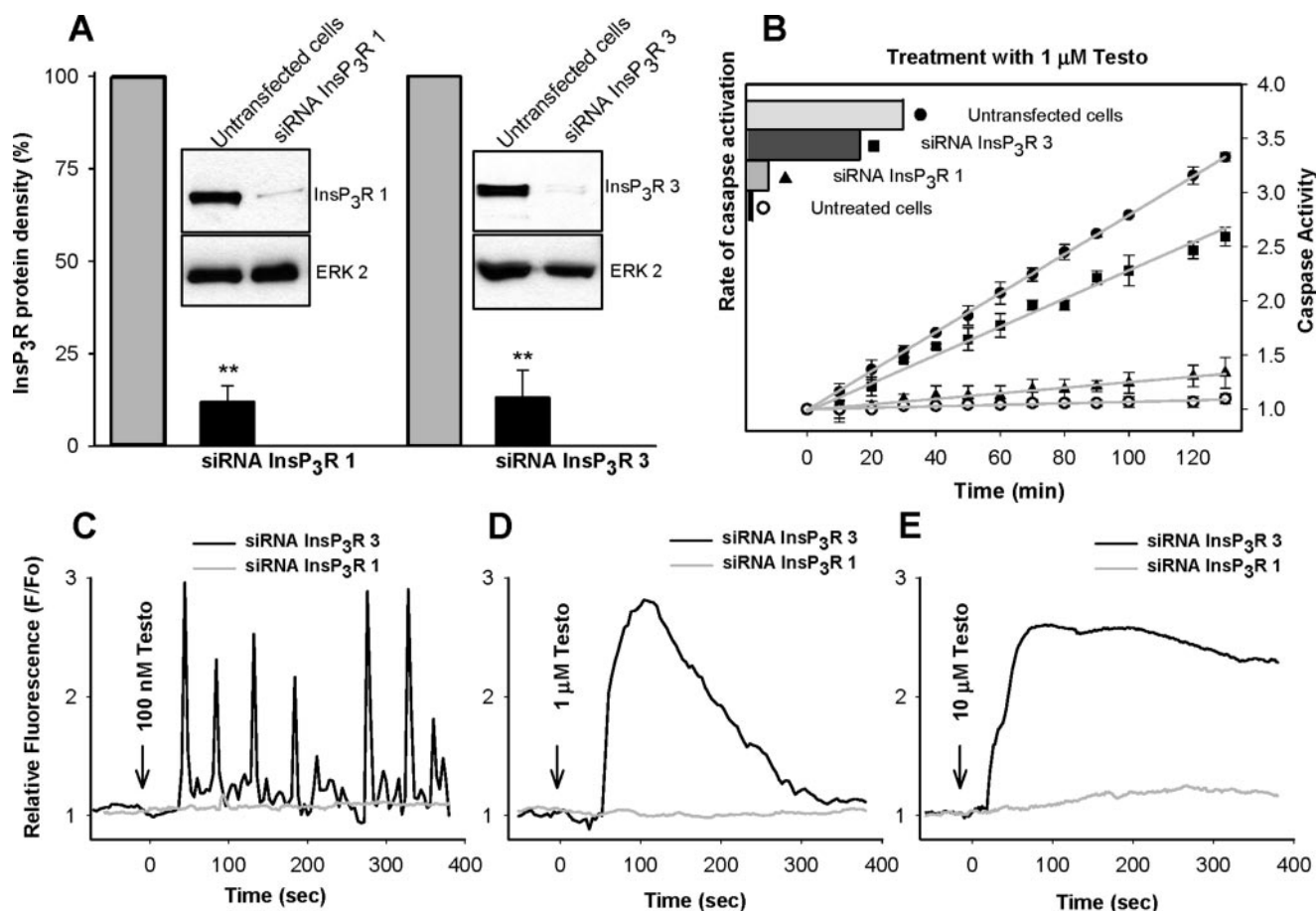


FIGURE 6. InsP₃R type 1 regulates Ca²⁺ signaling and apoptosis in response to testosterone (Testo). *A*, cells transiently transfected with InsP₃R-siRNA for either type 1 (*left*) or type 3 (*right*) showed a significant reduction (>80%) in the immunosignal. *B*, in InsP₃R type 1 siRNA-transfected cells, the caspase activity was inhibited (▲), whereas knockdown of InsP₃R type 3 had little effect on the caspase activity (■) in response to testosterone. Quantification of the rates of caspase activity in each of the conditions tested is shown in the *inset*. *C*, the response to testosterone in InsP₃R-siRNA-transfected cells depended upon the isoform of the InsP₃R that was decreased. Knockdown of the InsP₃R type 1 blocked the testosterone-induced Ca²⁺ signals at all three concentrations of testosterone tested (*gray lanes*). Knockdown of the InsP₃R type 3 did not modify the response to testosterone compared with untransfected cells (*black lanes*; see Fig. 4). The *arrows* indicate the time of the addition of the hormone. **, *p* < 0.01.

events, such as neurite outgrowth (12). In several cell models and using different apoptotic stimuli, it has been shown that an intracellular Ca²⁺ increase can trigger apoptosis (23, 25). In general, this occurs when the Ca²⁺ signal differs from the pattern expected for a specific stimulus. For example, modifying the amplitude or duration of the Ca²⁺ signals can lead to cell death (28). Here we show that testosterone can induce concentration-dependent patterns of Ca²⁺ signals. At low concentrations (100 nM), testosterone produces intracellular Ca²⁺ oscillations, which could be an important physiological mechanism for the action of androgen in neurons. When the concentration of testosterone is increased, the oscillatory pattern is lost, and transient and long-lasting responses appear. These testosterone-induced, long lasting rises in intracellular Ca²⁺ signals would be sufficient to initiate the apoptotic response.

Recently, a mechanism of apoptosis has been proposed that involves an interaction between cytochrome *c* and the InsP₃R (46, 47). It has been suggested that the release of cytochrome *c* from mitochondria into the cytosol during the early stages of apoptosis could induce changes in inositol 1,4,5-trisphosphate-mediated Ca²⁺ signals. The model relies upon a binding

between cytochrome *c* and the InsP₃R causing a lack of regulation and producing an exaggerated Ca²⁺ release from the endoplasmic reticulum (46–48). The results presented in this study are consistent with this model, which shows that InsP₃R blockers can inhibit the apoptotic response induced by testosterone. There are several reports that demonstrate that androgens can activate pertussis toxin-sensitive G proteins (49, 50). Also, other G-protein receptor agonists can induce an apoptotic program via phospholipase C-InsP₃R-Ca²⁺ increase. For example, G-protein activation and subsequent interaction of Gβγ with phospholipase C mediates the proapoptotic effects of ethanol in developing neural crest (51). The proapoptotic effects of the hormone angiotensin II also has been shown to mediate Ca²⁺ release from internal stores via G-protein-coupled receptor (52). Moreover, overexpression of wild-type Gα_q, which further increased G_q signaling, produced initial hypertrophy in cardiomyocytes, which rapidly progressed to apoptotic death (53).

Moreover, the importance of the InsP₃R pathway for cell survival has been shown in cell models where deletion of InsP₃R is associated with less cellular damage and more resistance to apoptosis (54, 55). Depending on the cell type studied, different subtypes of InsP₃R have been associated with apoptosis pro-

gression. In developing and regenerating neurons, InsP₃R type 1 is concentrated in the growth cone, suggesting its participation in neurite outgrowth (56), whereas InsP₃R type 3 has been shown to be in neuron terminals in limbic and basal forebrain regions, including olfactory tubercle, central nucleus of the amygdala, and bed nucleus of the stria terminalis (26). Elevated expression of InsP₃R type 3 has been implicated in developmental apoptosis in many cell types like early postnatal cerebellar granule cells, dorsal root ganglia, embryonic hair follicles, and intestinal villi (57). Recently, InsP₃R type 3 was shown to modulate apoptosis in epithelial cells (58). In contrast, InsP₃R type 1 was required for activation of the apoptosis pathway in T cells (54, 55) and in the neuroblastoma cells studied in this report. There are increasing numbers of reports showing differential distribution and different roles of InsP₃Rs (59, 60) in agreement with the hypothesis that specific isoforms of the InsP₃R will be critical for maintaining cell health; in the case of testosterone, the deleterious effects appear to be mediated through InsP₃R type 1.

Both beneficial and pathological effects of androgens are observed clinically. Depletion of androgen (below normal plasma levels) increases kainate-induced neuronal loss (61). Interestingly, high levels of testosterone also produced serious side effects and have been related to neurobehavioral changes like hyperexcitability, supra-aggressive nature, and suicidal tendencies (17, 18). Externally administered supraphysiological levels of testosterone can stimulate muscular bulk in human subjects (14, 15). Although this effect could be useful for patients with muscular physiopathologies, these kind of studies generally use blood testosterone concentrations ranging from 0.1 to 0.5 mM (16). Despite the complexity of the blood-brain barrier, the lipid-permeable nature of testosterone and the duration of these treatments (more than weeks) suggest that significant amounts of this hormone would be accessible to neuronal tissues. The effects of testosterone we describe here at the single cell level will have long term effects at the system level. Importantly, this study suggests that androgen supplementation for additional performance, rather than clinical needs, requires a careful reexamination. Thus, it appears that the beneficial effects of androgens are carefully regulated over a narrow (nanomolar) range of concentration, which is crucial for normal neuronal functions. A deviation from this concentration range in either direction could be deleterious for neuronal health.

The rapid effects of testosterone on intracellular Ca²⁺ signaling in neurons occur in the absence of the androgen receptor (12). There are additional effects of testosterone in neurons that require the androgen receptor (62). For example, testosterone activation of the androgen receptor increases the expression of cytoskeleton proteins, such as tubulin (63) and neuritin (64), which are important for neurite outgrowth and neuronal differentiation. Mutations of the androgen receptor that cause aggregation of polyglutamine-expanded protein induce cytotoxicity with normal levels of testosterone (65, 66), a primary cause of Kennedy syndrome (67). The effect of high testosterone concentration on cell function in these altered cells is not known. In addition, specific regions of the central nervous system contain 5 α -reductase, a key protein for the action of testosterone (68),

suggesting that in some cases local concentrations of testosterone could be higher than the plasma concentrations. Moreover, differential expression of androgen receptor in the central nervous system could also generate a range of testosterone sensitivity among neuronal cells (5).

Together, these results suggest that elevated concentrations of testosterone can induce programmed cell death, which is characterized by a decrease of cell viability, an increase in the number of annexin V-positive cells, DNA fragmentation, and caspase activation. Apoptotic parameters are blocked or diminished by InsP₃R inhibitors and the specific knocking down of InsP₃R type 1, indicating that this isoform is a key regulator in this event. Overall, the conclusions from these studies are that normal levels of testosterone are necessary for the normal Ca²⁺ response and to maintain homeostasis, but elevated concentrations produce altered Ca²⁺ signal, leading to deleterious effects in neurons.

Acknowledgments—We are grateful to M. Nathanson for providing critical reagents and to C. Gibson for thoughtful discussions and comments on the manuscript.

REFERENCES

- Gould, E., and McEwen, B. S. (1993) *Curr. Opin. Neurobiol.* **3**, 676–682
- McEwen, B. S. (1972) *Adv. Behav. Biol.* **4**, 41–59
- McEwen, B. S. (1997) *Ann. N. Y. Acad. Sci.* **823**, 201–213
- Pfaff, D. W., and McEwen, B. S. (1983) *Science* **219**, 808–814
- Kerr, J. E., Allore, R. J., Beck, S. G., and Handa, R. J. (1995) *Endocrinology* **136**, 3213–3221
- Sar, M., Lubahn, D. B., French, F. S., and Wilson, E. M. (1990) *Endocrinology* **127**, 3180–3186
- Hammond, J., Le, Q., Goodyer, C., Gelfand, M., Trifiro, M., and LeBlanc, A. (2001) *J. Neurochem.* **77**, 1319–1326
- Matsumoto, A., Arai, Y., Urano, A., and Hyodo, S. (1994) *Horm. Behav.* **28**, 357–366
- Rubinow, D. R., and Schmidt, P. J. (1996) *Am. J. Psychiatry* **153**, 974–984
- Tabori, N. E., Stewart, L. S., Znamensky, V., Romeo, R. D., Alves, S. E., McEwen, B. S., and Milner, T. A. (2005) *Neuroscience* **130**, 151–163
- Mong, J. A., Glaser, E., and McCarthy, M. M. (1999) *J. Neurosci.* **19**, 1464–1472
- Estrada, M., Uhlen, P., and Ehrlich, B. E. (2005) *J. Cell Sci.* **119**, 733–743
- Goldberg, J. L., and Barres, B. A. (2000) *Annu. Rev. Neurosci.* **23**, 579–612
- Bhasin, S., Storer, T. W., Berman, N., Callegari, C., Clevenger, B., Phillips, J., Bunnell, T. J., Tricker, R., Shirazi, A., and Casaburi, R. (1996) *N. Engl. J. Med.* **335**, 1–7
- Morales, A. J., Haubrich, R. H., Hwang, J. Y., Asakura, H., and Yen, S. S. (1998) *Clin. Endocrinol.* **49**, 421–432
- Rhoden, E. L., and Morgentaler, A. (2004) *N. Engl. J. Med.* **350**, 482–492
- Thiblin, I., Lindquist, O., and Rajs, J. (2000) *J. Forensic Sci.* **45**, 16–23
- Tirassa, P., Thiblin, I., Agren, G., Vigneti, E., Aloe, L., and Stenfors, C. (1997) *J. Neurosci. Res.* **47**, 198–207
- Strasser, A., O'Connor, L., and Dixit, V. M. (2000) *Annu. Rev. Biochem.* **69**, 217–245
- Thorburn, A. (2004) *Cell. Signal.* **16**, 139–144
- Bhuyan, A. K., Varshney, A., and Mathew, M. K. (2001) *Cell Death Differ.* **8**, 63–69
- Eldadah, B. A., and Faden, A. I. (2000) *J. Neurotrauma* **17**, 811–829
- Hajnoczky, G., Davies, E., and Madesh, M. (2003) *Biochem. Biophys. Res. Commun.* **304**, 445–454
- Orrenius, S., Zhivotovsky, B., and Nicotera, P. (2003) *Nat. Rev. Mol. Cell Biol.* **4**, 552–565
- Lipton, S. A., and Nicotera, P. (1998) *Cell Calcium* **23**, 165–171
- Sharp, A. H., Nucifora, F. C., Jr., Blondel, O., Sheppard, C. A., Zhang, C.,

- Snyder, S. H., Russell, J. T., Ryugo, D. K., and Ross, C. A. (1999) *J. Comp. Neurol.* **406**, 207–220
27. Guo, Q., Sopher, B. L., Furukawa, K., Pham, D. G., Robinson, N., Martin, G. M., and Mattson, M. P. (1997) *J. Neurosci.* **17**, 4212–4222
28. Verkhatsky, A., and Toescu, E. C. (2003) *J. Cell Mol. Med.* **7**, 351–361
29. Varshney, A., and Ehrlich, B. E. (2003) *Neuron* **39**, 195–197
30. Tang, T. S., Tu, H., Chan, E. Y., Maximov, A., Wang, Z., Wellington, C. L., Hayden, M. R., and Bezprozvanny, I. (2003) *Neuron* **39**, 227–239
31. Tang, T. S., Slow, E., Lupu, V., Stavrovskaya, I. G., Sugimori, M., Llinas, R., Kristal, B. S., Hayden, M. R., and Bezprozvanny, I. (2005) *Proc. Natl. Acad. Sci. U. S. A.* **102**, 2602–2607
32. Estrada, M., Liberona, J. L., Miranda, M., and Jaimovich, E. (2000) *Am. J. Physiol.* **279**, E132–E139
33. Nagata, S. (2005) *Annu. Rev. Immunol.* **23**, 853–875
34. Martin, S. J., and Green, D. R. (1995) *Cell* **82**, 349–352
35. Wojcikiewicz, R. J. (1995) *J. Biol. Chem.* **270**, 11678–11683
36. Tovey, S. C., de Smet, P., Lipp, P., Thomas, D., Young, K. W., Missiaen, L., De Smedt, H., Parys, J. B., Berridge, M. J., Thuring, J., Holmes, A., and Bootman, M. D. (2001) *J. Cell Sci.* **114**, 3979–3989
37. Mendes, C. C., Gomes, D. A., Thompson, M., Souto, N. C., Goes, T. S., Goes, A. M., Rodrigues, M. A., Gomez, M. V., Nathanson, M. H., and Leite, M. F. (2005) *J. Biol. Chem.*
38. Beato, M. (1989) *Cell* **56**, 335–344
39. Mooradian, A. D., Morley, J. E., and Korenman, S. G. (1987) *Endocr. Rev.* **8**, 1–28
40. Kelly, S. J., Ostrowski, N. L., and Wilson, M. A. (1999) *Pharmacol. Biochem. Behav.* **64**, 655–664
41. Aragno, M., Parola, S., Brignardello, E., Mauro, A., Tamagno, E., Manti, R., Danni, O., and Boccuzzi, G. (2000) *Diabetes* **49**, 1924–1931
42. Compagnone, N. A., and Mellon, S. H. (1998) *Proc. Natl. Acad. Sci. U. S. A.* **95**, 4678–4683
43. Freeman, L. M., Watson, N. V., and Breedlove, S. M. (1996) *Horm. Behav.* **30**, 424–433
44. Duval, D., Durant, S., and Homo-Delarche, F. (1983) *Biochim. Biophys. Acta* **737**, 409–442
45. Wozniak, A., Hutchison, R. E., Morris, C. M., and Hutchison, J. B. (1998) *Steroids* **63**, 263–267
46. Boehning, D., Patterson, R. L., Sedaghat, L., Glebova, N. O., Kurosaki, T., and Snyder, S. H. (2003) *Nat. Cell Biol.* **5**, 1051–1061
47. Boehning, D., Patterson, R. L., and Snyder, S. H. (2004) *Cell Cycle* **3**, 252–254
48. Boehning, D., van Rossum, D. B., Patterson, R. L., and Snyder, S. H. (2005) *Proc. Natl. Acad. Sci. U. S. A.* **102**, 1466–1471
49. Lieberherr, M., and Grosse, B. (1994) *J. Biol. Chem.* **269**, 7217–7223
50. Estrada, M., Espinosa, A., Muller, M., and Jaimovich, E. (2003) *Endocrinology* **144**, 3586–3597
51. Garic-Stankovic, A., Hernandez, M. R., Chiang, P. J., Debelak-Kragtorp, K. A., Flentke, G. R., Armant, D. R., and Smith, S. M. (2005) *Alcohol. Clin. Exp. Res.* **29**, 1237–1246
52. Kajstura, J., Cigola, E., Malhotra, A., Li, P., Cheng, W., Meggs, L. G., and Anversa, P. (1997) *J. Mol. Cell. Cardiol.* **29**, 859–870
53. Adams, J. W., Sakata, Y., Davis, M. G., Sah, V. P., Wang, Y., Liggett, S. B., Chien, K. R., Brown, J. H., and Dorn, G. W., II (1998) *Proc. Natl. Acad. Sci. U. S. A.* **95**, 10140–10145
54. Jayaraman, T., and Marks, A. R. (1997) *Mol. Cell. Biol.* **17**, 3005–3012
55. Szalai, G., Krishnamurthy, R., and Hajnoczky, G. (1999) *EMBO J.* **18**, 6349–6361
56. Takei, K., Shin, R. M., Inoue, T., Kato, K., and Mikoshiba, K. (1998) *Science* **282**, 1705–1708
57. Blackshaw, S., Sawa, A., Sharp, A. H., Ross, C. A., Snyder, S. H., and Khan, A. A. (2000) *FASEB J.* **14**, 1375–1379
58. Minagawa, N., Kruglov, E. A., Dranoff, J. A., Robert, M. E., Gores, G. J., and Nathanson, M. H. (2005) *J. Biol. Chem.* **280**, 33637–33644
59. Jochenning, F. W., Wenk, M. R., Uhlen, P., Degray, B., Lee, E., De Camilli, P., and Ehrlich, B. E. (2004) *Biochem. J.* **382**, 687–694
60. Jacob, S. N., Choe, C. U., Uhlen, P., DeGray, B., Yeckel, M. F., and Ehrlich, B. E. (2005) *J. Neurosci.* **25**, 2853–2864
61. Ramsden, M., Shin, T. M., and Pike, C. J. (2003) *Neuroscience* **122**, 573–578
62. Yerramilli-Rao, P., Garofalo, O., Whatley, S., Leigh, P. N., and Gallo, J. M. (1995) *J. Neurol. Sci.* **129**, (suppl.) 131–135
63. Matsumoto, A., Arai, Y., and Hyodo, S. (1993) *J. Neuroendocrinol.* **5**, 357–363
64. Marron, T. U., Guerini, V., Rusmini, P., Sau, D., Brevini, T. A., Martini, L., and Poletti, A. (2005) *J. Neurochem.* **92**, 10–20
65. Darrington, R. S., Butler, R., Leigh, P. N., McPhaul, M. J., and Gallo, J. M. (2002) *Neuroreport* **13**, 2117–2120
66. LaFevre-Bernt, M. A., and Ellerby, L. M. (2003) *J. Biol. Chem.* **278**, 34918–34924
67. Greenland, K. J., and Zajac, J. D. (2004) *Intern. Med. J.* **34**, 279–286
68. Frye, C. A., Edinger, K. L., Seliga, A. M., and Wawrzycki, J. M. (2004) *Psychoneuroendocrinology* **29**, 1019–1027